analytical chemistry

pubs.acs.org/ac Article

Boosting Detection of Low-Abundance Proteins in Thermal Proteome Profiling Experiments by Addition of an Isobaric Trigger Channel to TMT Multiplexes

Sarah A. Peck Justice, Neil A. McCracken, José F. Victorino, Guihong D. Qi, Aruna B. Wijeratne, and Amber L. Mosley*

Cite This: *Anal. Chem.* 2021, 93, 7000−7010 Read Online

ACCESS | Metrics & More | Article Recommendations | Supporting Information

ABSTRACT: The study of low-abundance proteins is a challenge to discovery-based proteomics. Mass spectrometry (MS) applications, such as thermal proteome profiling (TPP), face specific challenges in the detection of the whole proteome as a consequence of the use of nondenaturing extraction buffers. TPP is a powerful method for the study of protein thermal stability, but quantitative accuracy is highly dependent on consistent detection. Therefore, TPP can be limited in its amenability to study low-abundance proteins that tend to have stochastic or poor detection by MS. To address this challenge, we incorporated an affinity-purified protein complex sample at submolar concentrations as an isobaric trigger channel into a mutant TPP (mTPP) workflow to provide reproducible detection and quantitation of the low-abundance subunits of the cleavage and polyadenylation factor (CPF) complex. The inclusion of an isobaric protein complex trigger channel increased detection an average of 40× for previously detected subunits and facilitated detection of CPF subunits that were previously below the limit of detection. Importantly, these gains in CPF detection did not cause large changes in melt temperature (T_m) calculations for other unrelated proteins in the samples, with a high positive correlation between T_m estimates in samples with and without isobaric trigger channel addition. Overall, the incorporation of an affinity-purified protein complex as an isobaric trigger channel within a tandem mass tag (TMT) multiplex for mTPP experiments is an effective and reproducible way to gather thermal profiling data on proteins that are not readily detected using the original TPP or mTPP protocols.

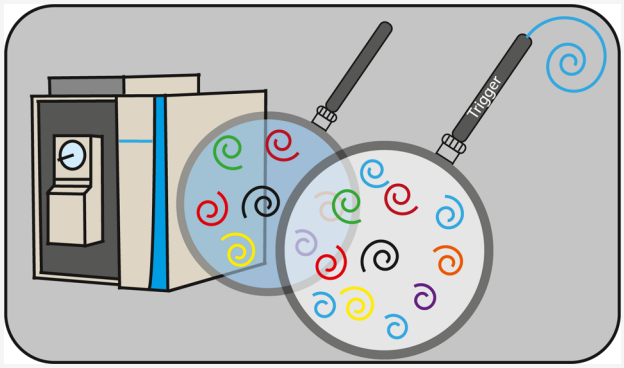

Proteins are the functional units of a cell, carrying out and controlling processes at specific times and locations to maintain homeostasis and respond to external stimuli. As a consequence of functional changes, proteins can exist in a variety of biophysical states within cells as a consequence of variants in their primary sequence, post-translational modification (PTM) state, and/or subcellular localization. In many cases, a protein's biophysical state is impacted by associations with other proteins, including both transient and stable protein−protein interactions. The characterization of protein−protein interactions (PPIs) is fundamental to gaining a full understanding of biological mechanisms. In fact, PPIs are so critical to proper protein function that gain or loss of interactions can lead to disease and/or cell death.[1,2] Advances in mass spectrometry (MS)-based proteomics workflows continue to increase our ability to study protein complex dynamics and PPIs.[3−8] MS-based approaches for protein interaction analysis rely on discovery-based proteomics performed using data-dependent acquisition (DDA). Generally in DDA, peptides with the most intense ions from MS^1 are selected for fragmentation and MS^2 analysis.[9] This approach maximizes signal-to-noise levels and thereby increases confidence in the selection and subsequent identification of the peptide ions.

Challenges with the use of DDA include the selection of peptide ions from protein(s) of interest that are present at low relative abundance levels or when peptides of interest (such as PTM containing peptides) are present at low relative levels to their unmodified counterparts. Low-abundance peptides may be present at insufficient MS^1 signal intensity levels to trigger fragmentation and MS^2 analysis based on instrument settings for MS^2 analysis. While fractionation and an extended high-performance liquid chromatography (HPLC) gradient help to spread out the elution of peptides into the mass spectrometer,

Received: January 2, 2021
Accepted: April 16, 2021
Published: April 28, 2021

many peptides may still coelute such that highly abundant ion species will outcompete those that are less abundant.[10] A number of strategies have recently emerged to improve MS detection of low-abundance proteins and post-translational modifications (PTMs) for a variety of applications including single-cell proteomics.[11−17] Although we will not discuss all of the recently established strategies here, one such strategy, boosting to amplify the signal with isobaric labeling (BASIL), has similarities that have informed the current work. Specifically, BASIL has been shown to successfully increase detection of low-abundance phosphopeptides through the addition of a boosting sample to a tandem mass tag (TMT)-based multiplex.[18] TMTPro labeling allows for the multiplexing and relative quantitation of up to 16 samples.[19−21] As each TMT label is isobaric, labeled peptides from the multiplexed samples elute into the mass spectrometer together and are analyzed simultaneously as one ion peak during MS^1 scans which are distinguished in fragment ion scans during MS^n (typically MS^2 or MS^3) analysis. By incorporating a phospho-enriched sample into a single channel in the TMT multiplex, Yi et al. increased ion abundance of phosphopeptides in the MS^1 scan to the extent that MS^2 was triggered for phosphopeptides that were typically below the level of detection in standard DDA approaches.[18] BASIL allowed for the identification and quantification of phosphopeptides in other TMT channels, where enrichment had not been performed.[18] The BASIL method has since been optimized for detection of phosphopeptides in single cells[22] and similar approaches have been applied to phosphotyrosine-containing peptides,[23] stable isotope labeling using amino acids in cell culture (SILAC)-labeled peptides,[24] and using synthetic peptides to particular peptides of interest.[25] BASIL and other similar methods that take advantage of isobaric carrier channels could have numerous applications in DDA-based quantitative workflows.

The challenges to studying low-abundance proteins in DDA proteomic experiments extend in particular to the mass spectrometry-based thermal proteome profiling (TPP) methods and are the focus of this study. TPP analysis takes advantage of TMT labeling technology to produce protein melt curves that can then be compared across conditions to measure alterations in protein thermal stability.[26,27] Although TPP was originally developed to study drug and ligand binding, it has also been shown to be a robust approach to probe PPIs in a number of different applications (recently reviewed by Mateus et al.[28]). We recently developed a new application of TPP referred to as mutant TPP (mTPP), which is used to study the effects of protein missense mutations on the proteome at large with the ability to focus on specific protein complexes and their PPIs.[29] mTPP analysis is advantageous over other methods for the study of PPIs in that it does not require antibodies, reagents such as crosslinkers, or production of fusion proteins. Additionally, mTPP can be performed with significantly less starting material than traditional affinity purification or enrichment approaches, making it applicable to a wider variety of sample types. Despite these advantages, we have encountered challenges associated with quantitative analysis of specific target proteins and their interaction partners. Detection of low-abundance target proteins is inherent to many DDA-based proteomic studies because of the large dynamic range of eukaryotic proteomes such that analysis of a global proteome results in excellent quantitation of high-abundance proteins, while the majority of the proteome is surveyed in a more stochastic manner at both the protein and peptide levels.[30] One advantage of TMT- and isobaric tag for relative and absolute quantitation (iTRAQ)-based multiplexed workflows for global proteomics studies is that the pooling of multiple samples generates increased protein starting material that can then be subjected to extensive biochemical fractionation to facilitate deep proteome coverage.[31−35] This advantage can be coupled with protein extraction methods using denaturants such as urea or sodium dodecyl sulfate (SDS) to isolate the full proteome of many cells and tissues.[36] The workflow for TPP cannot exploit these advantages since (1) temperature treatment of lysates for TPP results in unequal levels of protein mixture across the multiplex that, in our hands, vary on average at least 10-fold from the lowest to the highest temperature treatment[29] and (2) nondenaturing protein extraction buffers must be used to maintain protein structure, PPIs, and protein interactions with other molecules (including but not limited to lipids, metabolites, small molecules, and drugs).[26−28] As a consequence, TPP workflows typically result in decreased proteome coverage relative to denaturant extracted proteomes even when equivalent amounts of starting material are used.[29]

We have developed a BASIL-like approach that expands proteome coverage for our mTPP workflow and increases the signal of low-abundance protein complexes and their representative peptides. Our mTPP experiment approach uses a protein complex affinity purification trigger channel in place of the phosphopeptide isobaric boosting channel used in BASIL.[18] As a proof-of-concept, we investigated the ability of this approach to enhance detection of the relatively low-abundance protein complex cleavage and polyadenylation factor (CPF) complex in a mTPP workflow. Affinity-purified CPF that we previously characterized[37−41] was incorporated as an isobaric trigger channel in our mTPP workflow at a ratio to the lowest heat-treated mTPP sample of ∼1:8 and ∼1:50. Using this approach, we observed a significant increase in the abundance of CPF complex members, including those that were not readily identified without the isobaric trigger channel. Importantly, the addition of an isobaric trigger channel into our mTPP workflow did not appear to have a significant impact on the calculated melt temperature (T_m) of proteins detected. Overall, the use of an isobaric trigger channel is a robust approach for prioritizing DDA selection of low-abundance proteins or peptides of interest such as missense mutant-containing proteins and their interaction partners, which are of particular focus within mTPP experiments.

EXPERIMENTAL SECTION

Yeast Strains and Growth. All experiments were performed in *Saccharomyces cerevisiae*. The parental strain SMY732[42] was obtained from the Mirkin Lab and used in the trigger experiments comparing technical replicates. For the biological replicate experiments, the wild-type strain used was *BY4741* (Open Biosystems). The *ssu72-2* temperature-sensitive mutant[43] was from Euroscarf. The Pta1-FLAG strain was made via homologous recombination. The 3xFLAG tag DNA sequence was amplified from plasmids obtained from Funakoshi and Hochstrasser[44] to insert the FLAG epitope tag into the genome at the 3′-end of the *PTA1* gene in wild type (WT) (BY4741). Successful incorporation of the FLAG tag was confirmed via Western blot. For mTPP experiments, cells were grown as previously described.[29]

https://doi.org/10.1021/acs.analchem.1c00012
Anal. Chem. 2021, 93, 7000−7010

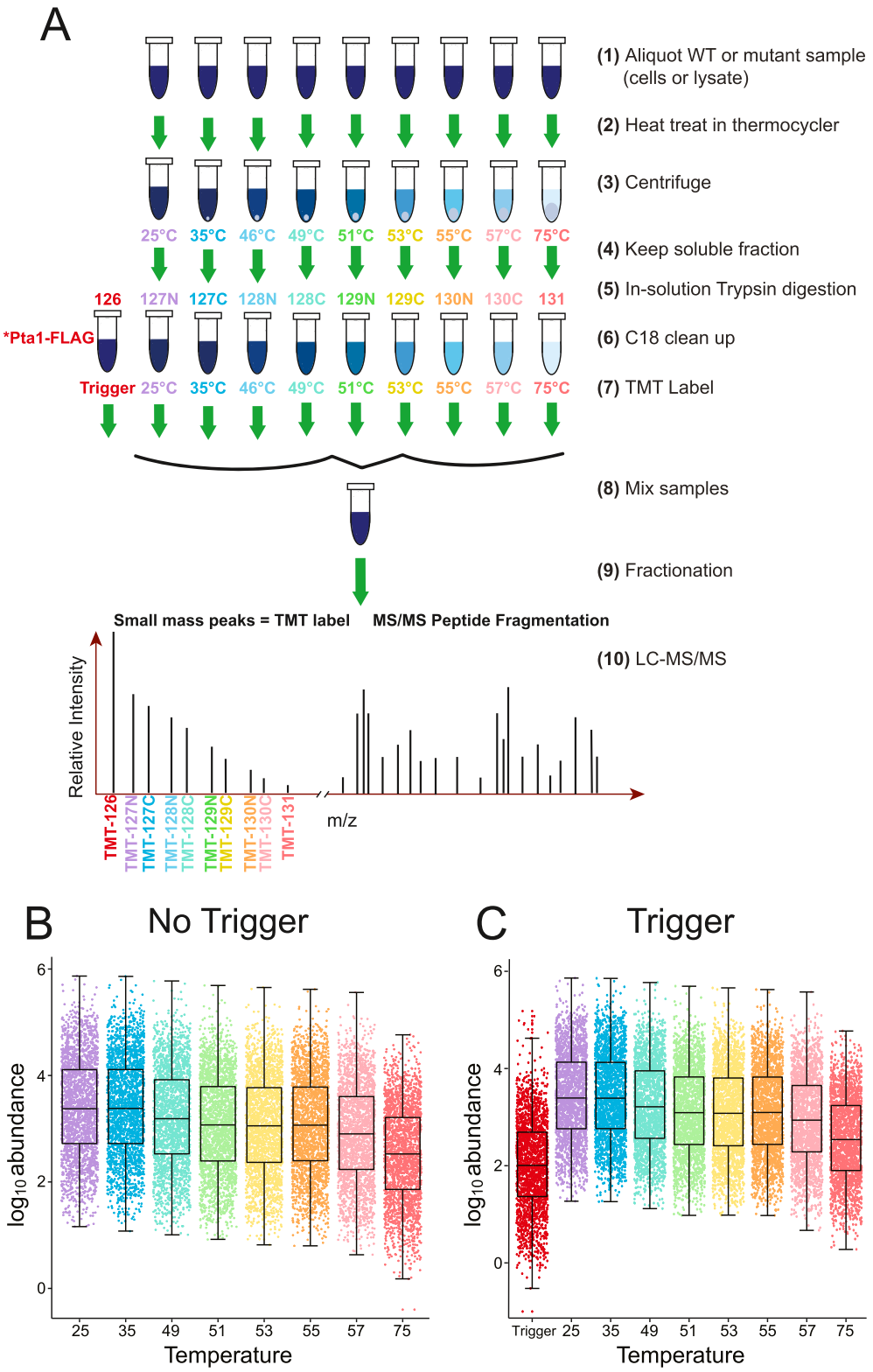

Figure 1. Workflow overview for mTPP with isobaric trigger channel addition. (A) Equal amounts of protein from each lysate for every biological replicate sample were subjected to different temperature treatments to induce protein denaturation. The soluble fractions from each treatment as well as a Pta1-FLAG affinity purification sample were digested in solution with trypsin/Lys-C. The resulting peptides were labeled with isobaric mass tags (TMT 10plex) as shown and mixed prior to mass spectrometry (MS) analysis. Resulting tandem mass spectrometry (MS/MS) data were analyzed using Proteome Discoverer 2.4 to identify and quantify abundance levels of peptides for each temperature treatment and each biological replicate across genotypes. The dot plots of protein-abundance values for each protein detected in WT cells in technical replicates without (B) and with (C) the isobaric trigger channel (trigger) addition.

Sample Preparation. BY4741 and *ssu72-2* samples for mTPP were prepared as described in Peck Justice et al.[29] with an extended temperature range for the heat treatment. The lysate was treated at the following 10 temperatures: untreated,

https://doi.org/10.1021/acs.analchem.1c00012
Anal. Chem. 2021, 93, 7000−7010

25, 35, 46.2, 48.8, 51.2, 53.2, 55.2, 56.5, and 74.9 °C. A TMT 10plex kit (Thermo Scientific, Waltham, MA) was used to label each sample as shown in Figure 1. SMY732 lysate was treated at the following eight temperatures: 25, 35, 48.8, 51.2, 53.2, 55.2, 56.5, and 74.9 °C. A TMT 16plex kit (Thermo Scientific, Waltham, MA) was used to label peptide solutions derived from each temperature treatment, as shown in Figure S1. Note that some channels in the 16plex were used for other samples not described in this report. TMT labeling steps were performed according to manufacturer-provided instructions.

Affinity purification of native CPF via Pta1-FLAG was performed as described previously for Ssu72-FLAG purifications.[37] The Pta1-FLAG affinity-purified sample was added at a ratio of 6.25 μg trigger to 50 μg of the lowest heat-treated sample (1:8 ratio) for the biological replicates. The untreated samples were removed from the multiplex from no trigger samples to accommodate for the isobaric trigger channel to be labeled with TMT126. Technical replicate samples were divided and multiplexed into two separate mixes. In one experiment, the set of combined labeled samples was analyzed with a ninth trigger channel (TMT126) at a ratio of 1 μg total isobaric trigger channel protein to 50 μg of the lowest heat-treated sample (1:50 ratio), which included the Pta1-FLAG affinity-purified material, while in the second experiment, the trigger was not added. Subsequent sample preparation steps were performed as described.[28] The ratio of trigger channel protein to experimental samples (based on the lowest temperature sample concentration) was well below the 1:0.02−1:0.05 ratios reported to be successful for accurate quantitation for low cell/single-cell studies.[45,46]

LC-MS/MS Analysis. Following multiplex preparation, samples were subjected to high-pH reversed-phase fractionation.[29] NanoLC-MS/MS analyses were performed on an Orbitrap Fusion Lumos mass spectrometer coupled to an EASY-nLC HPLC (Thermo Scientific, Waltham, MA). One-third of the fractions were loaded onto an Easy-Nano 25 cm column with 2 μm reversed-phase resin. The peptides were eluted using a 180 min gradient increasing from 95% buffer A (0.1% formic acid in water) and 5% buffer B (0.1% formic acid in acetonitrile) to 25% buffer B at a flow rate of 400 nL/min. The peptides were eluted using a 180 min gradient increasing from 95% buffer A (0.1% formic acid in water) and 5% buffer B (0.1% formic acid in acetonitrile) to 25% buffer B at a flow rate of 400 nL/min. MS data was acquired using data-dependent acquisition (DDA) using a top speed method following the first survey MS scan. During MS^1, using a wide quadrupole isolation, survey scans were obtained with an Orbitrap resolution of 120k with vendor-defined parameters—m/z scan range, 375−1500; maximum injection time, 50; automatic gain control (AGC) target, 4×10^5; micro scans, 1; and RF lens (%), 30. During MS^2, the following parameters were assigned to isolate and fragment the selected precursor ions: isolation window = 0.7; FirstMass = 120; activation type = higher-energy collisional dissociation (HCD); and collision energy (%) = 38; the data were recorded using Thermo Scientific Xcalibur (4.1.31.9) software.

Protein Identification and Quantification. The resulting RAW files were analyzed using Proteome Discoverer 2.4 (Thermo Scientific, Waltham, MA). The SEQUEST HT search engine was used to search against a yeast protein database from the UniProt sequence database containing 6279 yeast protein and common contaminant sequences (FASTA file used available on ProteomeXchange under accession PXD020689). Specific search parameters used were trypsin as the proteolytic enzyme, peptides with a max of two missed cleavages, precursor mass tolerance of 10 ppm, and a fragment mass tolerance of 0.02 Da. Static modifications were (1) carbamidomethylation on cysteine; (2) TMTsixplex label on lysine (K) and the N-termini of peptides. Dynamic modifications were the oxidation of methionine and acetylation of N-termini. Percolator false discovery rate (FDR) was set to a strict setting of 0.01. Values from both unique and razor peptides were used for quantification. The mass spectrometry proteomic data have been deposited to the ProteomeXchange Consortium via the PRIDE[47] partner repository with the data set identifier PXD020689 and doi: 10.6019/PXD020689. The impurity adjustments supplied within the TMT kit from Thermo Scientific were also accounted for in the analysis to limit the impact of TMT channel crosstalk.

Data Analysis. Venn diagrams were created using Venny 2.1.[48] Dot plots, scatter plots, and waterfall plots were created using ggplot2[49] in R Studio (R Studio for Mac, version 1.2.5001). Bar graphs were created in Excel (version 16.38). The TPP package (v3.12.0)[50] in R Studio was used to generate normalized melt curves and to determine protein melt temperatures as described previously.[27] Resulting data processing and analysis also occurred in R Studio. Changes in melt temperature (T_m), ΔT_m values, were calculated by taking WT T_m -*ssu72-2* T_m, thereby limiting calculations to proteins detected in both WT and mutant. Further parsing was accomplished by limiting our data to melt curves with r^2 values >0.9 and then by proteins that were detected in at least two of the three replicates. Changes in T_m that were outside of $\pm 2\sigma$ (σ being the standard deviation) were considered statistically significant and identified as proteins destabilized or stabilized due to the mutations in *SSU72*. Gene ontology (GO) enrichment analysis was performed using the publicly available Gene Ontology Resource.[51,52]

RESULTS AND DISCUSSION

Addition of an Affinity-Purified Isobaric Trigger Channel to mTPP Multiplexes Does Not Cause Large Changes in Peptide Coverage or Quantitation. We hypothesized that incorporation of a well-characterized affinity-purified sample isolated from our system of interest as an isobaric trigger channel would increase MS^1 ion intensity of peptides of interest within the TMT multiplex. As a consequence, the identification of peptides from the affinity-purified native protein complex would boost the identification in the remaining experimental mTPP channels used for melt curve production and subsequent T_m calculation when comparing different experimental samples. The incorporation of an affinity-purified CPF complex purified from our system of interest has numerous potential advantages, similar to the approach used in BASIL,[18] including native levels of CPF processing events, post-translational modifications, and protein interaction partners. Affinity purifications for the CPF complex were performed in a manner similar to mTPP using nondenaturing buffers to preserve PPIs. Qualitatively, the MS/MS fragment data for CPF complexes would also be improved from the inclusion of the isobaric trigger channel increasing the ion abundance of the fragments and therefore the probability of CPF identification at the peptide spectrum match (PSM) level. From a quantitative perspective, TMT126 information is obtained during data processing but is excluded for interpretation of the mTPP melt curves for each protein.

https://doi.org/10.1021/acs.analchem.1c00012
Anal. Chem. 2021, 93, 7000−7010

A

	Technical Replicates		Biological Replicates			
	No trigger	Trigger	No trigger	Trigger p1	Trigger p2	Trigger p3
# total PSMs	178,199	180,013	188,000	96,211	144,119	143,690
# total peptide groups	28,608	25,685	38,673	18,085	34,354	34,732
# proteins identified	2,797	2,650	3,339	1,994	3,097	3,095
# proteins quantified	2,309	2,209	3,149	1,751	2,903	2,874
# proteins with melt curve $r^2 > 0.9$	2,185	2,093	2,983	1,648	2,786	2,655

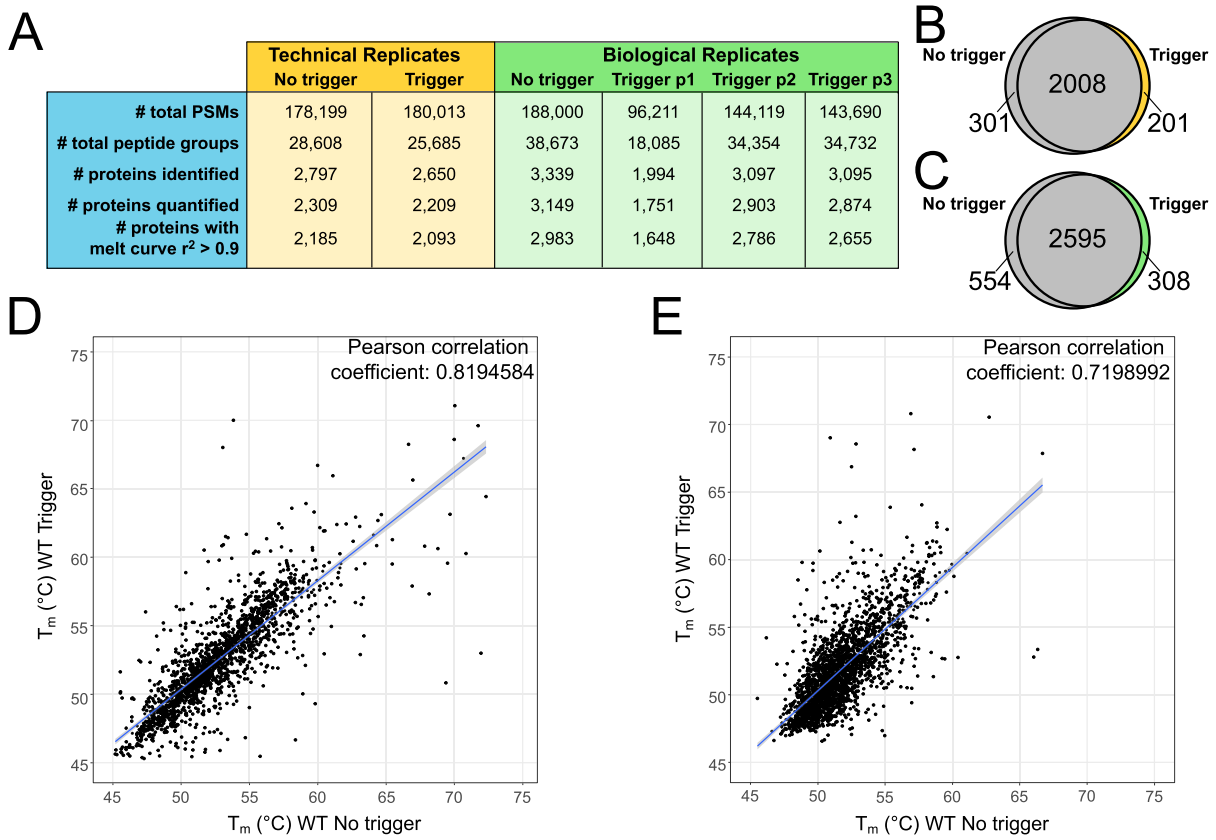

Figure 2. Data set comparisons from isobaric trigger channel addition. (A) Summary of LC-MS/MS data in technical and biological replicates with and without isobaric trigger channel addition. Venn diagrams comparing quantified proteins in no trigger (gray) vs trigger (yellow/green) in (B) technical replicates and (C) biological replicate using trigger p2. Correlation plot of the calculated T_ms in no trigger vs trigger in (D) technical replicates and (E) biological replicates. The blue line represents the linear fit of the data.

Pta1-3xFLAG affinity purifications were digested with Lys-C/trypsin and labeled with TMT126 for inclusion within the mTPP multiplex. mTPP quantitative analysis and curve generation was performed using the remaining channels as described in the methods (Figure 1A). The mTPP samples were subjected to eight or nine different temperatures and then centrifuged to separate soluble and insoluble material as previously described.[29] For samples with eight temperature points no 46.2° treatment sample was included. Samples were then processed and subjected to LC-MS/MS analysis using an MS^2-based fragmentation and TMT quantitation workflow (Figure 1). Between 1750 and 3150, proteins were detected and quantified depending on the replicate (Table S1) when using SEQUEST HT and Proteome Discoverer 2.4 for qualitative and quantitative analysis. Replicates are designated as preparation 1, 2, 3 (hence p1, p2, p3). The p1 replicate had fewer IDs overall but p2 and p3 had very similar peptide detection levels (Table S1). Dot plots were generated to show the abundance value for each quantified protein and to gain insights into general trends with the quantitative data (Figures 1B,C and S2). Consistent with previous mTPP experiments,[29] there was an overall decrease in protein abundance as the temperature at which the sample was treated increased. Importantly, incorporation of a protein complex isobaric trigger channel into the multiplex did not alter the overall trend of decreasing protein abundance with increased temperature or have a significant effect on the number of proteins detected. The average ion abundance at each temperature treatment also remained consistent between samples with and without the isobaric trigger channel suggesting that there were no significant levels of TMT channel crosstalk from the inclusion of the CPF trigger (compare abundance distributions between Figure 1B,C). The average quantitative ratio of the isobaric trigger channel to the mTPP experimental sample processed at 25 °C remains consistent at a 1:50 (Figure 1C) or 1:8 (Figure S2), reflecting the ratios used for mixing of the multiplex.

The impact of the trigger on mTPP analysis was investigated using both technical replicates and biological replicates so that we could evaluate differences in our workflow and their impact on qualitative and quantitative parameters. Technical replicate analyses showed very similar numbers of detected PSMs, peptides, and proteins suggesting that the addition of the trigger channel at a ratio of 1:50 has little impact on overall LC-MS/MS detection (Figure 2A, yellow). While there was not an obvious effect on the overall abundance of proteins in the samples, it is possible that the trigger could affect the detection and identification of proteins by biasing the mass spectrometer toward proteins present in the affinity purification. Comparisons of MS-based measurements across the technical replicates showed that the trigger channel incorporation did not have a significant impact on protein identification and quantification (Figure 2A). The biological replicates showed more variation across samples which is attributed to their separate processing for TPP in addition to variation that could occur from trypsin digestion and other processing steps.[53,54] Trigger p1 in the biological replicate study did have overall lower levels of proteins detected, but

https://doi.org/10.1021/acs.analchem.1c00012
Anal. Chem. 2021, 93, 7000−7010

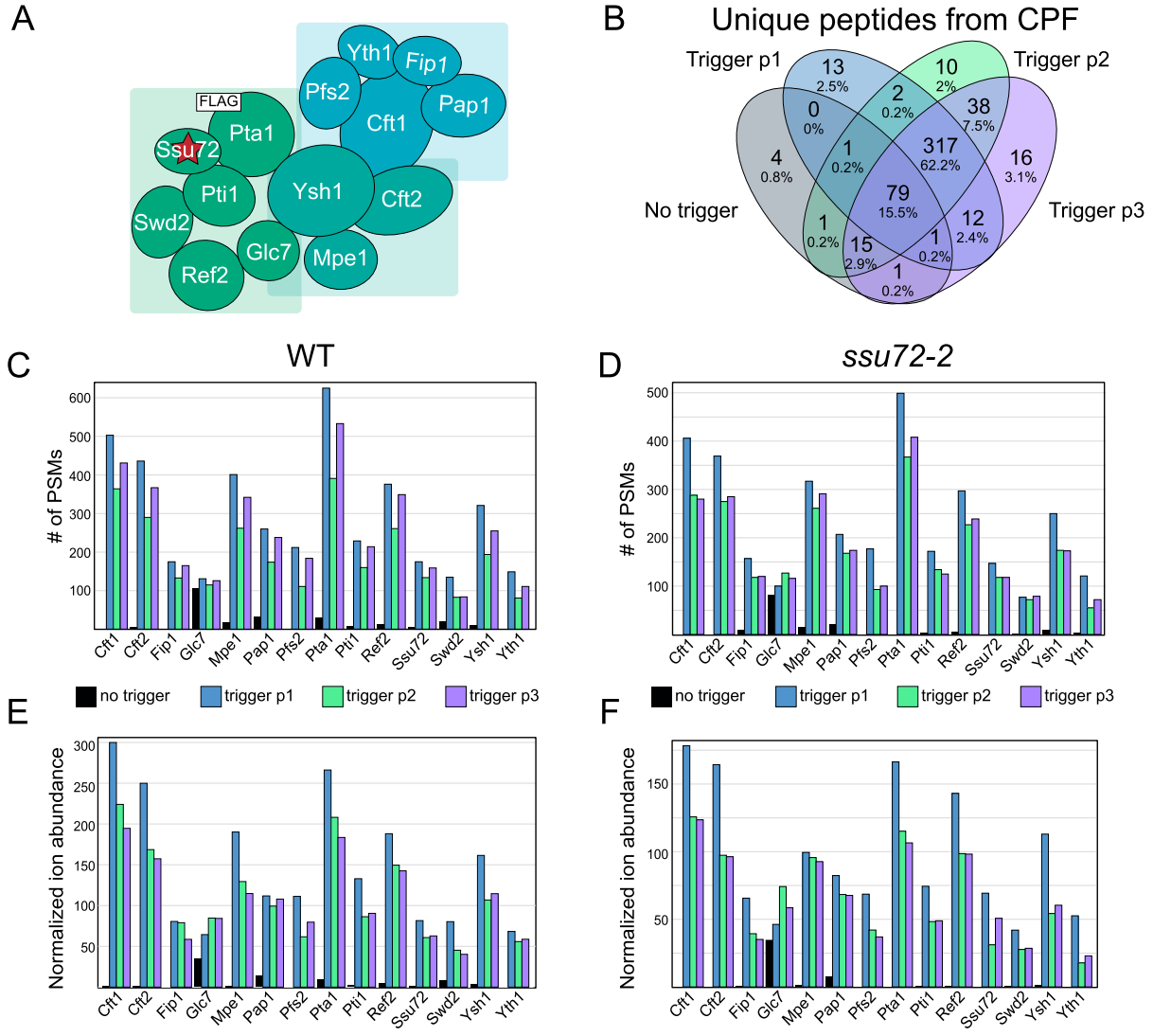

Figure 3. Peptide detection and quantitation for subunits of the cleavage and polyadenylation factor complex present in the Pta1-FLAG isobaric trigger channel. (A) Model of CPF adapted from Casañal et al.[59] The red star denotes the mutant protein used in these studies, *ssu72-2*; the white square denotes the FLAG-tagged subunit used for the trigger channel affinity purification, Pta1. (B) Venn diagram showing the unique peptides detected for CPF subunits across each WT biological replicate. Number of PSMs for CPF subunits in each (C) WT and (D) *ssu72-2* replicate experiment. Ion abundance for CPF subunits normalized to the abundance of Pgk1 (1000×) in each (E) WT and (F) *ssu72-2* replicate experiment.

this was not likely a consequence of trigger channel addition considering that trigger p2 and trigger p3 samples had similar detection levels to the no trigger sample (Figure 2A, green). Direct comparison of proteins quantified in the no trigger vs trigger samples showed an 80% overlap in quantified proteins with unique proteins present in all individual data sets (Figure 2B,C). Overall, these data suggest that the addition of an isobaric trigger channel has little to no impact on overall proteome detection outside of the inherent variability seen in independent sample processing (for the biological replicates) and LC-MS/MS runs.

A critical feature of mTPP analysis is the ability to accurately calculate melt temperature (T_m) from the resulting melt curves. To ensure that incorporation of the trigger did not have major impacts on T_m calculation of proteins outside of the CPF complex, we performed Pearson correlation analysis of the protein melt temperatures detected in both the no trigger and trigger samples (Figure 2D, T_m data from the TPP package in Table S2). From these, we can see a high degree of correlation of 0.82 between the no trigger and trigger samples for proteins, which met the criteria for quantitation in our mTPP data analysis workflow (including the number of proteins with melt curves having an r^2 greater than or equal to 0.9). Additionally, even across biological replicates, there is a strong positive correlation of 0.72 between T_m calculations in the no trigger vs trigger samples (Figure 2E, T_m data from the TPP package in Table S2). The ability to make comparisons using biological replicate data would be beneficial in scenarios with limiting samples where technical replicates may not be feasible. Biological replicates are also important for rigorous statistical analysis.

Isobaric Trigger Channel Facilitates mTPP Analysis of the Cleavage and Polyadenylation Factor Complex. CPF and its accessory factors cleavage factor IA and IB play major roles in RNA processing. CPF is responsible for efficient and specific cleavage and polyadenylation of messenger RNAs[55,56] and has been shown to have important roles in termination of RNA Polymerase II transcription.[57,58] The CPF complex is currently described as having 14 subunits (Figure 3A) which provide the complex with numerous activities

https://doi.org/10.1021/acs.analchem.1c00012
Anal. Chem. 2021, 93, 7000−7010

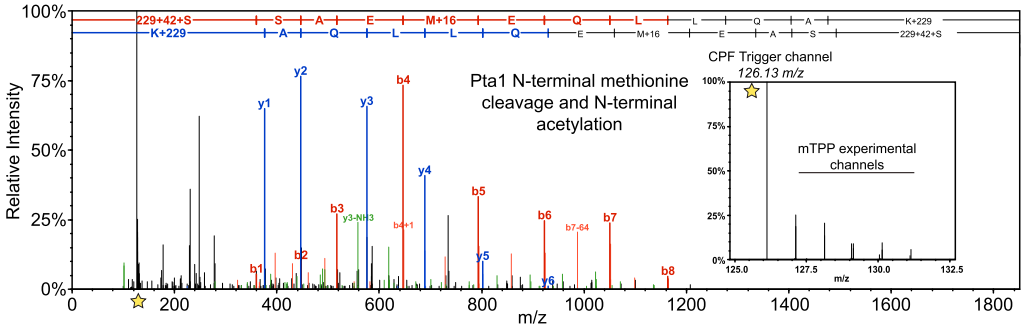

Figure 4. CPF trigger channel allows for reproducible detection of protein processing and amino acid modifications. MS^2 fragment ion spectrum for Pta1 N-terminus. TMT reporter ions are indicated with a star (left) with a close-up view of the CPF trigger channel signal relative to the mTPP experimental data shown to the right.

including endonuclease, polyadenylation, and phosphatase functions.[59] Ssu72, which is mutated in the *ssu72-2* yeast strain, is an integral subunit of CPF (Figure 3A, indicated with a star). Performing mTPP according to the established protocol[29] resulted in limited detection of the CPF (Figure 3C−F). One notable exception to the low detection of CPF when no trigger was used was the subunit Glc7. Along with its presence in CPF, Glc7 is also the catalytic subunit of PP1[60] and thereby functions in many other protein complexes in eukaryotic cells (reviewed in refs 61 and 62), where it plays roles in cell cycle regulation and nutrient regulation.[60,63] Glc7 has a higher global abundance than other CPF subunits and is thereby more readily detected.

We have previously shown that PSM level detection of affinity-purified protein complexes results in highly reproducible quantitation of protein complexes in label-free quantitation workflows.[40,41] This prior work found that RNA polymerase II complex digestions result in the generation of a number of highly detectable peptides and it is likely that this would also be the case for CPF affinity purifications.[41] If these findings hold true, there should be a significant overlap in unique peptide identifications across the independent LC-MS/MS runs for biological replicates. As shown in Figure 3B, a significant overlap of unique peptides from CPF subunits was identified across the three biological replicates containing the isobaric CPF trigger (peptide data provided in Table S4). These findings clearly show that the use of a high-purity affinity purification as an isobaric trigger channel can facilitate reproducible quantitation of over 300 unique peptides. Considering that DDA of eukaryotic proteomes can often lead to stochastic peptide selection from low-abundance proteins, these data show that the CPF trigger channel can increase analytical measurement precision through reproducible peptide selection for MS^2. From an individual subunit perspective, incorporation of the isobaric Pta1-FLAG trigger channel significantly increased the identification of most CPF subunits substantially (Figure 3C−F). Some CPF subunits that were previously not detected in no trigger samples (such as Cft1, Cft2, and Pfs2) were represented by hundreds of PSMs by utilizing the isobaric CPF trigger channel (Figure 3C,D). The increased level of PSM detection was accompanied by increased normalized ion abundance (Figure 3E,F).

Of note, Pta1-FLAG purifications are isolated from yeast that have been engineered to express Pta1-FLAG at native levels resulting in the purification of CPF complexes which have biologically relevant stoichiometry, protein processing, and protein post-translational modification(s). The CPF trigger channel also facilitated mTPP analysis of CPF subunit cotranslational modifications such as N-terminal methionine cleavage and acetylation of the new N-terminus (serine 2 in the protein database, Figure 4). Post-translational modification events such as phosphorylation of Pti1 at serine 272 were also reproducibly measured in CPF trigger mTPP experiments (Figure S5). These data show that the use of native protein complex purifications as an isobaric trigger channel has the unique advantage of triggering tandem MS analysis of peptides representing various biologically relevant proteoforms. Additionally, manual inspection of the ratio of the trigger channel abundance (126) to the lowest temperature abundance within the mTPP channels revealed that the amount of CPF peptides needed for boosting to allow for reproducible quantitation ranged between <2 and 5-fold (Figures 4 and S5).

Mutations in *ssu72-2* Do Not Impact the Thermal Stability of the CPF Protein Complex. The CPF complex contains two protein phosphatases, Glc7 and Ssu72. Ssu72 is an integral component of CPF and its function is required for proper termination and 3′-end processing of RNAs.[64−67] Additionally, its interactions with TFIIB have shown to be critical for the formation of gene loops, which regulate gene expression by linking transcription termination and initiation factors.[68−71] Much of the characterization of Ssu72 has been accomplished through studies using the *ssu72-2* mutant yeast strain.[43,64] The *ssu72-2* TS mutant contains a single mutation, R129A, that confers temperature sensitivity at 37 °C. This mutation impairs the catalytic activity of Ssu72, leading to a decrease in transcription elongation efficiency and defects in gene looping.[69,71] Whether or not the missense mutation in the *ssu72-2* cells affects the thermal stability of the Ssu72/CPF complex has not been previously examined and is required to make a conclusion about if the ssu72-2 causes a protein-specific change in activity that causes the phenotype or if it causes a protein complex-specific change (such as instability or poor assembly) that could alter the activity or recruitment of other CPF subunits.

Detection of CPF with and without the trigger channel resulted in similar numbers of CPF subunit PSMs in *ssu72-2* as in WT, which facilitates mTPP analysis of CPF complex thermal stability from a quantitative perspective (Figure 4C,D). Protein melt curve analysis using the TPP R package (Figure 5A, mTPP result data in Table S3) showed no obvious changes in any of the 14 CPF subunits in *ssu72-2* relative to WT. We have defined statistically significant changes in protein thermal stability as any ΔT_m, which fall at least two standard deviations above or below the average ΔT_m across the three

https://doi.org/10.1021/acs.analchem.1c00012
Anal. Chem. 2021, 93, 7000−7010

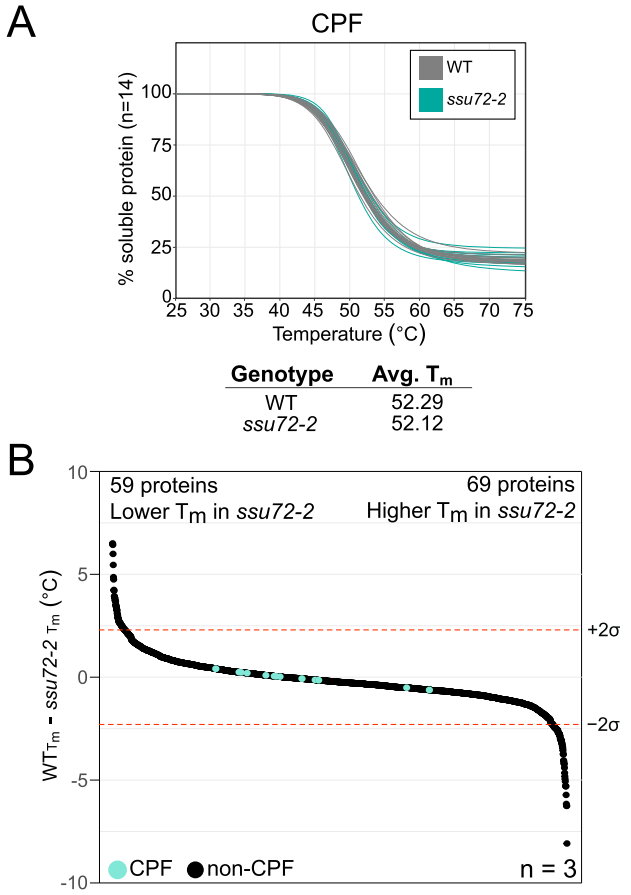

Figure 5. Effects of *ssu72-2* on CPF complex stability and the global proteome. (A) mTPP is normalized CPF subunit melt curves. Plots for each of the CPF subunits are normalized by the TPP package for a representative replicate, trigger p2. The curves shown in gray are WT and turquoise are *ssu72-2*. Each line represents one of the 14 CPF subunits. Replicates for (A) are provided in Figure S5. (B) Waterfall plots visualizing whole proteome changes in melt temperature (T_m), WT- *ssu72-2*. Median values are shown for proteins that are quantified in at least two replicates. The dotted lines signify a confidence interval of 95%. There are significant decreases in the thermal stability of 59 proteins and significant increases in 69 proteins. Change in T_m and median values are provided in Table S5.

ssu72-2 replicates relative to WT. Whole proteome analysis of ΔT_m using mTPP found statistically significant decreases in the thermal stability of 59 proteins and increases in the thermal stability of 69 proteins in *ssu72-2* cells (Figure 5B and Table S5). GO term analysis[72] of proteins that had a significant change in thermal stability in *ssu72-2* showed a 2.40-fold enrichment in proteins involved in the nucleobase-containing compound biosynthetic process with a *p*-value of 4.14×10^{-5}. These results suggest that the defects in transcription caused by the disrupted catalytic activity of Ssu72 in this mutant strain are not due to impacts on the stability of Ssu72 or stability or the assembly of the CPF complex. Secondary effects of *ssu72-2* have been associated with changes in the Nrd1−Nab3−Sen1 complex activity that impacts a variety of processes including GTP production.[67,73,74] The temperature sensitivity of this strain is more likely to be a result of a need for efficient transcription at higher temperatures to respond to heat stress.[75,76] A deeper investigation into the proteins with changes in thermal stability will help to further elucidate the impacts of this catalytic mutant on gene expression.

CONCLUSIONS

The integration of an isobaric affinity-purified protein complex trigger channel increased our ability to analyze the thermal stability of the low-abundance protein complex CPF via mTPP. Our analysis did not observe major changes on the T_m estimates of unrelated proteins, suggesting that an affinity-purified isobaric trigger channel is a robust analytical approach for measurement of low-abundance protein mTPP analysis. CPF protein complex digestion results in the detection of a highly reproducible peptide population which will support precise measurement of low-abundance protein melt curves for proteins of interest while still obtaining survey information about the proteome at large. The use of natively expressed purifications from the system of interest, however, has distinct advantages including native protein processing, post-translational modifications, and protein interaction partners.

The use of isobaric purified protein complex trigger channels in TPP studies, and potentially other global proteomics applications, will improve the ability to perform proteomic analysis of low-abundance protein complexes with analytical reproducibility and precision to measure systems-level perturbations due to genetic variation(s). The potential for this method to be used across different organisms, even those that are difficult to get large amounts of protein from, is further supported by the adaptation of BASIL for single-cell phosphoproteomics.[22] As many biologically relevant, as well as disease relevant, protein complexes are of relatively low abundance in the cell,[77] improvements in the reproducible detection of such proteins in proteomics experiments would be beneficial to increasing our understanding of the critical cellular mechanisms in normal and disease states (Supporting Information).

ASSOCIATED CONTENT

Supporting Information

The Supporting Information is available free of charge at https://pubs.acs.org/doi/10.1021/acs.analchem.1c00012.

TMT channels used for each sample (Figure S1); WT protein-abundance dot plots (Figure S2); *ssu72-2* protein-abundance dot plots (Figure S3); unique CPF peptide detection (Figure S4); Pti1 phosphorylation detection with CPF trigger channel (Figure S5); PSMs and ion-abundance measurements for CPF subunits in WT technical replicates (Figure S6); and Replicate CPF melt curves (Figure S7) (PDF)

mTPP data (Table S1) (XLSX)

TPP package results, WT no trigger vs WT trigger (Table S2) (XLSX)

TPP package results, WT vs *ssu72-2* (Table S3) (XLSX)

Peptide groups for CPF subunits in WT and *ssu72-2* (Table S4) (XLSX)

Changes in T_m and median changes (Table S5) (XLSX)

AUTHOR INFORMATION

Corresponding Author

Amber L. Mosley − *Department of Biochemistry and Molecular Biology, Indiana University School of Medicine, Indianapolis, Indiana 46202, United States;* orcid.org/0000-0001-5822-2894; Phone: (317) 278-2350; Email: almosley@iu.edu; Fax: (317) 274-4686

https://doi.org/10.1021/acs.analchem.1c00012
Anal. Chem. 2021, 93, 7000−7010

Authors

Sarah A. Peck Justice − *Department of Biochemistry and Molecular Biology, Indiana University School of Medicine, Indianapolis, Indiana 46202, United States*

Neil A. McCracken − *Department of Biochemistry and Molecular Biology, Indiana University School of Medicine, Indianapolis, Indiana 46202, United States*

José F. Victorino − *Department of Biochemistry and Molecular Biology, Indiana University School of Medicine, Indianapolis, Indiana 46202, United States*

Guihong D. Qi − *Department of Biochemistry and Molecular Biology, Indiana University School of Medicine, Indianapolis, Indiana 46202, United States*

Aruna B. Wijeratne − *Department of Biochemistry and Molecular Biology, Indiana University School of Medicine, Indianapolis, Indiana 46202, United States*

Complete contact information is available at: https://pubs.acs.org/10.1021/acs.analchem.1c00012

Author Contributions

S.A.P.J. designed and performed mTPP experiments, analyzed data, prepared the figures, and wrote the manuscript. N.A.M. performed mTPP experiments and contributed to the manuscript. J.F.V. incorporated affinity-purified CPF and confirmed purification via AP-MS (data shown elsewhere). A.B.W. contributed to the design of experiments. A.L.M. oversaw various aspects of the project, designed mTPP experiments, provided funding, provided direction on data analysis, and wrote the manuscript. The manuscript was written through contributions of all authors. All authors have given approval to the final version of the manuscript.

Notes

The authors declare no competing financial interest.

■ ACKNOWLEDGMENTS

We would like to thank all of the members of the Mosley Lab and IUSM Proteomics Core for their helpful discussions and support for this project. Funding was provided by NIH R01 GM099714 (A.L.M.), NIH T32 HL007910 (S.A.P.J.), and the Showalter Research Trust (A.L.M.). N.A.M. was supported in part by the IU Diabetes and Obesity Research Training Program, DeVault Fellowship. This project was also supported, in part, with support from the Indiana Clinical and Translational Sciences Institute, which is funded by Award number UL1TR002529 from the NIH, NCATS Award. Acquisition of the IUSM Proteomic core instrumentation used for this project was provided by the Indiana University Precision Health Initiative. Some of the TMT reagents were graciously provided via the Thermo Scientific TMT Research Award (S.A.P.J.). The content is solely the responsibility of the authors and does not necessarily represent the official views of the NIH.

■ REFERENCES

(1) Sahni, N.; Yi, S.; Taipale, M.; Fuxman Bass, J. I.; Coulombe-Huntington, J.; Yang, F.; Peng, J.; Weile, J.; Karras, G. I.; Wang, Y.; Kovacs, I. A.; Kamburov, A.; Krykbaeva, I.; Lam, M. H.; Tucker, G.; Khurana, V.; Sharma, A.; Liu, Y. Y.; Yachie, N.; Zhong, Q.; Shen, Y.; Palagi, A.; San-Miguel, A.; Fan, C.; Balcha, D.; Dricot, A.; Jordan, D. M.; Walsh, J. M.; Shah, A. A.; Yang, X.; Stoyanova, A. K.; Leighton, A.; Calderwood, M. A.; Jacob, Y.; Cusick, M. E.; Salehi-Ashtiani, K.; Whitesell, L. J.; Sunyaev, S.; Berger, B.; Barabasi, A. L.; Charloteaux, B.; Hill, D. E.; Hao, T.; Roth, F. P.; Xia, Y.; Walhout, A. J. M.; Lindquist, S.; Vidal, M. *Cell* **2015**, *161*, 647−660.

(2) Fragoza, R.; Das, J.; Wierbowski, S. D.; Liang, J.; Tran, T. N.; Liang, S.; Beltran, J. F.; Rivera-Erick, C. A.; Ye, K.; Wang, T. Y.; Yao, L.; Mort, M.; Stenson, P. D.; Cooper, D. N.; Wei, X.; Keinan, A.; Schimenti, J. C.; Clark, A. G.; Yu, H. *Nat. Commun.* **2019**, *10*, No. 4141.

(3) Huttlin, E. L.; Bruckner, R. J.; Paulo, J. A.; Cannon, J. R.; Ting, L.; Baltier, K.; Colby, G.; Gebreab, F.; Gygi, M. P.; Parzen, H.; Szpyt, J.; Tam, S.; Zarraga, G.; Pontano-Vaites, L.; Swarup, S.; White, A. E.; Schweppe, D. K.; Rad, R.; Erickson, B. K.; Obar, R. A.; Guruharsha, K. G.; Li, K.; Artavanis-Tsakonas, S.; Gygi, S. P.; Harper, J. W. *Nature* **2017**, *545*, 505−509.

(4) Chick, J. M.; Munger, S. C.; Simecek, P.; Huttlin, E. L.; Choi, K.; Gatti, D. M.; Raghupathy, N.; Svenson, K. L.; Churchill, G. A.; Gygi, S. P. *Nature* **2016**, *534*, 500−505.

(5) Gavin, A. C.; Bosche, M.; Krause, R.; Grandi, P.; Marzioch, M.; Bauer, A.; Schultz, J.; Rick, J. M.; Michon, A. M.; Cruciat, C. M.; Remor, M.; Hofert, C.; Schelder, M.; Brajenovic, M.; Ruffner, H.; Merino, A.; Klein, K.; Hudak, M.; Dickson, D.; Rudi, T.; Gnau, V.; Bauch, A.; Bastuck, S.; Huhse, B.; Leutwein, C.; Heurtier, M. A.; Copley, R. R.; Edelmann, A.; Querfurth, E.; Rybin, V.; Drewes, G.; Raida, M.; Bouwmeester, T.; Bork, P.; Seraphin, B.; Kuster, B.; Neubauer, G.; Superti-Furga, G. *Nature* **2002**, *415*, 141−147.

(6) Lambert, J. P.; Ivosev, G.; Couzens, A. L.; Larsen, B.; Taipale, M.; Lin, Z. Y.; Zhong, Q.; Lindquist, S.; Vidal, M.; Aebersold, R.; Pawson, T.; Bonner, R.; Tate, S.; Gingras, A. C. *Nat. Methods* **2013**, *10*, 1239−1245.

(7) Go, C. D.; Knight, J. D. R.; Rajasekharan, A.; Rathod, B.; Hesketh, G. G.; Abe, K. T.; Youn, J.-Y.; Samavarchi-Tehrani, P.; Zhang, H.; Zhu, L. Y.; Popiel, E.; Lambert, J.-P.; Coyaud, É.; Cheung, S. W. T.; Rajendran, D.; Wong, C. J.; Antonicka, H.; Pelletier, L.; Raught, B.; Palazzo, A. F.; Shoubridge, E. A.; Gingras, A.-C. *bioRxiv* **2019**, 1−31.

(8) Rolland, T.; Tasan, M.; Charloteaux, B.; Pevzner, S. J.; Zhong, Q.; Sahni, N.; Yi, S.; Lemmens, I.; Fontanillo, C.; Mosca, R.; Kamburov, A.; Ghiassian, S. D.; Yang, X.; Ghamsari, L.; Balcha, D.; Begg, B. E.; Braun, P.; Brehme, M.; Broly, M. P.; Carvunis, A. R.; Convery-Zupan, D.; Corominas, R.; Coulombe-Huntington, J.; Dann, E.; Dreze, M.; Dricot, A.; Fan, C.; Franzosa, E.; Gebreab, F.; Gutierrez, B. J.; Hardy, M. F.; Jin, M.; Kang, S.; Kiros, R.; Lin, G. N.; Luck, K.; MacWilliams, A.; Menche, J.; Murray, R. R.; Palagi, A.; Poulin, M. M.; Rambout, X.; Rasla, J.; Reichert, P.; Romero, V.; Ruyssinck, E.; Sahalie, J. M.; Scholz, A.; Shah, A. A.; Sharma, A.; Shen, Y.; Spirohn, K.; Tam, S.; Tejeda, A. O.; Trigg, S. A.; Twizere, J. C.; Vega, K.; Walsh, J.; Cusick, M. E.; Xia, Y.; Barabasi, A. L.; Iakoucheva, L. M.; Aloy, P.; De Las Rivas, J.; Tavernier, J.; Calderwood, M. A.; Hill, D. E.; Hao, T.; Roth, F. P.; Vidal, M. *Cell* **2014**, *159*, 1212−1226.

(9) Aebersold, R.; Mann, M. *Nature* **2016**, *537*, 347−355.

(10) Altelaar, A. F.; Munoz, J.; Heck, A. J. *Nat. Rev. Genet.* **2013**, *14*, 35−48.

(11) Meier, F.; Geyer, P. E.; Virreira Winter, S.; Cox, J.; Mann, M. *Nat. Methods* **2018**, *15*, 440−448.

(12) Potel, C. M.; Lin, M.-H.; Heck, A. J. R.; Lemeer, S. *Mol. Cell. Proteomics* **2018**, *17*, 1028−1034.

(13) Humphrey, S. J.; Azimifar, S. B.; Mann, M. *Nat. Biotechnol.* **2015**, *33*, 990−995.

(14) Specht, H.; Slavov, N. *J. Proteome Res.* **2020**, 880−887.

(15) Slavov, N. *Curr. Opin. Chem. Biol.* **2021**, *60*, 1−9.

(16) Zhu, Y.; Scheibinger, M.; Ellwanger, D. C.; Krey, J. F.; Choi, D.; Kelly, R. T.; Heller, S.; Barr-Gillespie, P. G. *Elife* **2019**, No. e50777.

(17) Budnik, B.; Levy, E.; Harmange, G.; Slavov, N. *Genome Biol.* **2018**, *19*, No. 161.

(18) Yi, L.; Tsai, C. F.; Dirice, E.; Swensen, A. C.; Chen, J.; Shi, T.; Gritsenko, M. A.; Chu, R. K.; Piehowski, P. D.; Smith, R. D.; Rodland, K. D.; Atkinson, M. A.; Mathews, C. E.; Kulkarni, R. N.; Liu, T.; Qian, W. J. *Anal. Chem.* **2019**, *91*, 5794−5801.

(19) McAlister, G. C.; Huttlin, E. L.; Haas, W.; Ting, L.; Jedrychowski, M. P.; Rogers, J. C.; Kuhn, K.; Pike, I.; Grothe, R. A.; Blethrow, J. D.; Gygi, S. P. *Anal. Chem.* **2012**, *84*, 7469−7478.
(20) Thompson, A.; Schafer, J.; Kuhn, K.; Kienle, S.; Schwarz, J.; Schmidt, G.; Neumann, T.; Hamon, C. *Anal. Chem.* **2003**, *75*, 1895−1904.
(21) Thompson, A.; Wolmer, N.; Koncarevic, S.; Selzer, S.; Bohm, G.; Legner, H.; Schmid, P.; Kienle, S.; Penning, P.; Hohle, C.; Berfelde, A.; Martinez-Pinna, R.; Farztdinov, V.; Jung, S.; Kuhn, K.; Pike, I. *Anal. Chem.* **2019**, *91*, 15941−15950.
(22) Tsai, C. F.; Zhao, R.; Williams, S. M.; Moore, R. J.; Schultz, K.; Chrisler, W. B.; Pasa-Tolic, L.; Rodland, K. D.; Smith, R. D.; Shi, T.; Zhu, Y.; Liu, T. *Mol. Cell. Proteomics* **2020**, *19*, 828−838.
(23) Chua, X. Y.; Mensah, T.; Aballo, T. J.; Mackintosh, S. G.; Edmondson, R. D.; Salomon, A. R. *Mol. Cell. Proteomics* **2020**, 730−743.
(24) Klann, K.; Tascher, G.; Munch, C. *Mol. Cell* **2020**, *77*, 913.e4−925.e4.
(25) Yamamoto, W. R.; Bone, R. N.; Sohn, P.; Syed, F.; Reissaus, C. A.; Mosley, A. L.; Wijeratne, A. B.; True, J. D.; Tong, X.; Kono, T.; Evans-Molina, C. *J. Biol. Chem.* **2019**, *294*, 168−181.
(26) Savitski, M. M.; Reinhard, F. B.; Franken, H.; Werner, T.; Savitski, M. F.; Eberhard, D.; Martinez Molina, D.; Jafari, R.; Dovega, R. B.; Klaeger, S.; Kuster, B.; Nordlund, P.; Bantscheff, M.; Drewes, G. *Science* **2014**, *346*, No. 1255784.
(27) Franken, H.; Mathieson, T.; Childs, D.; Sweetman, G. M.; Werner, T.; Togel, I.; Doce, C.; Gade, S.; Bantscheff, M.; Drewes, G.; Reinhard, F. B.; Huber, W.; Savitski, M. M. *Nat. Protoc.* **2015**, *10*, 1567−1593.
(28) Mateus, A.; Kurzawa, N.; Becher, I.; Sridharan, S.; Helm, D.; Stein, F.; Typas, A.; Savitski, M. M. *Mol. Syst. Biol.* **2020**, *16*, No. e9232.
(29) Peck Justice, S. A.; Barron, M. P.; Qi, G. D.; Wijeratne, H. R. S.; Victorino, J. F.; Simpson, E. R.; Vilseck, J. Z.; Wijeratne, A. B.; Mosley, A. L. *J. Biol. Chem.* **2020**, 16219−16238.
(30) Nagaraj, N.; Wisniewski, J. R.; Geiger, T.; Cox, J.; Kircher, M.; Kelso, J.; Paabo, S.; Mann, M. *Mol. Syst. Biol.* **2011**, *7*, 548.
(31) Batth, T. S.; Francavilla, C.; Olsen, J. V. *J. Proteome Res.* **2014**, *13*, 6176−6186.
(32) Wang, Y.; Yang, F.; Gritsenko, M. A.; Wang, Y.; Clauss, T.; Liu, T.; Shen, Y.; Monroe, M. E.; Lopez-Ferrer, D.; Reno, T.; Moore, R. J.; Klemke, R. L.; Camp, D. G., 2nd; Smith, R. D. *Proteomics* **2011**, *11*, 2019−2026.
(33) Mertins, P.; Tang, L. C.; Krug, K.; Clark, D. J.; Gritsenko, M. A.; Chen, L.; Clauser, K. R.; Clauss, T. R.; Shah, P.; Gillette, M. A.; Petyuk, V. A.; Thomas, S. N.; Mani, D. R.; Mundt, F.; Moore, R. J.; Hu, Y.; Zhao, R.; Schnaubelt, M.; Keshishian, H.; Monroe, M. E.; Zhang, Z.; Udeshi, N. D.; Mani, D.; Davies, S. R.; Townsend, R. R.; Chan, D. W.; Smith, R. D.; Zhang, H.; Liu, T.; Carr, S. A. *Nat. Protoc.* **2018**, *13*, 1632−1661.
(34) Hogrebe, A.; von Stechow, L.; Bekker-Jensen, D. B.; Weinert, B. T.; Kelstrup, C. D.; Olsen, J. V. *Nat. Commun.* **2018**, *9*, No. 1045.
(35) Gilar, M.; Olivova, P.; Daly, A. E.; Gebler, J. C. *Anal. Chem.* **2005**, *77*, 6426−6434.
(36) Ludwig, K. R.; Schroll, M. M.; Hummon, A. B. *J. Proteome Res.* **2018**, *17*, 2480−2490.
(37) Victorino, J. F.; Fox, M. J.; Smith-Kinnaman, W. R.; Peck Justice, S. A.; Burriss, K. H.; Boyd, A. K.; Zimmerly, M. A.; Chan, R. R.; Hunter, G. O.; Liu, Y.; Mosley, A. L. *PLoS Genet.* **2020**, *16*, No. e1008317.
(38) Bedard, L. G.; Dronamraju, R.; Kerschner, J. L.; Hunter, G. O.; Axley, E. D.; Boyd, A. K.; Strahl, B. D.; Mosley, A. L. *J. Biol. Chem.* **2016**, *291*, 13410−13420.
(39) Smith-Kinnaman, W. R.; Berna, M. J.; Hunter, G. O.; True, J. D.; Hsu, P.; Cabello, G. I.; Fox, M. J.; Varani, G.; Mosley, A. L. *Mol. BioSyst.* **2014**, *10*, 1730−1741.
(40) Mosley, A. L.; Hunter, G. O.; Sardiu, M. E.; Smolle, M.; Workman, J. L.; Florens, L.; Washburn, M. P. *Mol. Cell. Proteomics* **2013**, *12*, 1530−1538.
(41) Mosley, A. L.; Sardiu, M. E.; Pattenden, S. G.; Workman, J. L.; Florens, L.; Washburn, M. P. *Mol. Cell. Proteomics* **2011**, *10*, No. M110 000687.
(42) McGinty, R. J.; Puleo, F.; Aksenova, A. Y.; Hisey, J. A.; Shishkin, A. A.; Pearson, E. L.; Wang, E. T.; Housman, D. E.; Moore, C.; Mirkin, S. M. *Cell Rep.* **2017**, *20*, 2490−2500.
(43) Pappas, D. L.; Hampsey, M. *Mol. Cell. Biol.* **2000**, *20*, 8343−8351.
(44) Funakoshi, M.; Hochstrasser, M. *Yeast* **2009**, *26*, 185−192.
(45) Cheung, T. K.; Lee, C. Y.; Bayer, F. P.; McCoy, A.; Kuster, B.; Rose, C. M. *Nat. Methods* **2021**, *18*, 76−83.
(46) Dou, M.; Clair, G.; Tsai, C. F.; Xu, K.; Chrisler, W. B.; Sontag, R. L.; Zhao, R.; Moore, R. J.; Liu, T.; Pasa-Tolic, L.; Smith, R. D.; Shi, T.; Adkins, J. N.; Qian, W. J.; Kelly, R. T.; Ansong, C.; Zhu, Y. *Anal. Chem.* **2019**, *91*, 13119−13127.
(47) Perez-Riverol, Y.; Csordas, A.; Bai, J.; Bernal-Llinares, M.; Hewapathirana, S.; Kundu, D. J.; Inuganti, A.; Griss, J.; Mayer, G.; Eisenacher, M.; Pérez, E.; Uszkoreit, J.; Pfeuffer, J.; Sachsenberg, T.; Yılmaz, Ş.; Tiwary, S.; Cox, J.; Audain, E.; Walzer, M.; Jarnuczak, A. F.; Ternent, T.; Brazma, A.; Vizcaíno, J. A. *Nucleic Acids Res.* **2019**, *47*, D442−D450.
(48) Oliveros, J. C. Venny. An Interactive Tool for Comparing Lists with Venn's Diagrams, 2007−2015.
(49) Wickham, H. *ggplot2: Elegant Graphics for Data Analysis*; Springer-Verlag: New York, 2016.
(50) Childs, D.; Kurzawa, N.; Franken, H.; Doce, C.; Savitski, M.; Huber, W. *TPP: Analyze Thermal Proteome Profiling (TPP) Experiments*, R package version 3.10.0, 2018.
(51) Gene Ontology Consortium. *Nucleic Acids Res.* **2021**, *49*, D325−D334.
(52) Ashburner, M.; Ball, C. A.; Blake, J. A.; Botstein, D.; Butler, H.; Cherry, J. M.; Davis, A. P.; Dolinski, K.; Dwight, S. S.; Eppig, J. T.; Harris, M. A.; Hill, D. P.; Issel-Tarver, L.; Kasarskis, A.; Lewis, S.; Matese, J. C.; Richardson, J. E.; Ringwald, M.; Rubin, G. M.; Sherlock, G. *Nat. Genet.* **2000**, *25*, 25−29.
(53) Walmsley, S. J.; Rudnick, P. A.; Liang, Y.; Dong, Q.; Stein, S. E.; Nesvizhskii, A. I. *J. Proteome Res.* **2013**, *12*, 5666−5680.
(54) Burkhart, J. M.; Schumbrutzki, C.; Wortelkamp, S.; Sickmann, A.; Zahedi, R. P. *J. Proteomics* **2012**, *75*, 1454−1462.
(55) Chen, J.; Moore, C. *Mol. Cell. Biol.* **1992**, *12*, 3470−3481.
(56) Kessler, M. M.; Zhao, J.; Moore, C. L. *J. Biol. Chem.* **1996**, *271*, 27167−27175.
(57) Proudfoot, N. J. *Science* **2016**, *352*, No. aad9926.
(58) Eaton, J. D.; Davidson, L.; Bauer, D. L. V.; Natsume, T.; Kanemaki, M. T.; West, S. *Genes Dev.* **2018**, *32*, 127−139.
(59) Casañal, A.; Kumar, A.; Hill, C. H.; Easter, A. D.; Emsley, P.; Degliesposti, G.; Gordiyenko, Y.; Santhanam, B.; Wolf, J.; Wiederhold, K.; Dornan, G. L.; Skehel, M.; Robinson, C. V.; Passmore, L. A. *Science* **2017**, *358*, 1056−1059.
(60) Feng, Z. H.; Wilson, S. E.; Peng, Z. Y.; Schlender, K. K.; Reimann, E. M.; Trumbly, R. J. *J. Biol. Chem.* **1991**, *266*, 23796−23801.
(61) Martín, R.; Stonyte, V.; Lopez-Aviles, S. *Int. J. Mol. Sci.* **2020**, *21*, No. 395.
(62) Moura, M.; Conde, C. *Biomolecules* **2019**, *9*, No. 55.
(63) Ramaswamy, N. T.; Li, L.; Khalil, M.; Cannon, J. F. *Genetics* **1998**, *149*, 57−72.
(64) Dichtl, B.; Blank, D.; Ohnacker, M.; Friedlein, A.; Roeder, D.; Langen, H.; Keller, W. *Mol. Cell* **2002**, *10*, 1139−1150.
(65) Nedea, E.; He, X.; Kim, M.; Pootoolal, J.; Zhong, G.; Canadien, V.; Hughes, T.; Buratowski, S.; Moore, C. L.; Greenblatt, J. *J. Biol. Chem.* **2003**, *278*, 33000−33010.
(66) Steinmetz, E. J.; Brow, D. A. *Mol. Cell. Biol.* **2003**, *23*, 6339−6349.
(67) Zhang, D. W.; Mosley, A. L.; Ramisetty, S. R.; Rodriguez-Molina, J. B.; Washburn, M. P.; Ansari, A. Z. *J. Biol. Chem.* **2012**, *287*, 8541−8551.
(68) Ansari, A.; Hampsey, M. *Genes Dev.* **2005**, *19*, 2969−2978.

https://doi.org/10.1021/acs.analchem.1c00012
Anal. Chem. 2021, 93, 7000−7010

(69) Allepuz-Fuster, P.; O'Brien, M. J.; Gonzalez-Polo, N.; Pereira, B.; Dhoondia, Z.; Ansari, A.; Calvo, O. *Nucleic Acids Res.* **2019**, *47*, 8975−8987.
(70) Singh, B. N.; Hampsey, M. *Mol. Cell* **2007**, *27*, 806−816.
(71) Tan-Wong, S. M.; Zaugg, J. B.; Camblong, J.; Xu, Z.; Zhang, D. W.; Mischo, H. E.; Ansari, A. Z.; Luscombe, N. M.; Steinmetz, L. M.; Proudfoot, N. J. *Science* **2012**, *338*, 671−675.
(72) Mi, H.; Huang, X.; Muruganujan, A.; Tang, H.; Mills, C.; Kang, D.; Thomas, P. D. *Nucleic Acids Res.* **2017**, *45*, D183−D189.
(73) Ganem, C.; Devaux, F.; Torchet, C.; Jacq, C.; Quevillon-Cheruel, S.; Labesse, G.; Facca, C.; Faye, G. *EMBO J.* **2003**, *22*, 1588−1598.
(74) Loya, T. J.; O'Rourke, T. W.; Reines, D. *Nucleic Acids Res.* **2012**, *40*, 7476−7491.
(75) Mahat, D. B.; Salamanca, H. H.; Duarte, F. M.; Danko, C. G.; Lis, J. T. *Mol. Cell* **2016**, *62*, 63−78.
(76) Duarte, F. M.; Fuda, N. J.; Mahat, D. B.; Core, L. J.; Guertin, M. J.; Lis, J. T. *Genes Dev.* **2016**, *30*, 1731−1746.
(77) Ho, B.; Baryshnikova, A.; Brown, G. W. *Cell Syst.* **2018**, *6*, 192.e3−205.e3.

https://doi.org/10.1021/acs.analchem.1c00012
Anal. Chem. 2021, 93, 7000−7010